Spatially Dependent Transfer Functions for Web Lateral Dynamics in Roll-to-Roll Manufacturing

Edison O. Cobos Torres
Department of Mechanical Engineering,
Texas A & M University,
College Station, TX 77843
e-mail: orlando.cobos@tamu.edu

Prabhakar R. Pagilla[1]
Professor
Department of Mechanical Engineering,
Texas A & M University,
College Station, TX 77843
e-mail: ppagilla@tamu.edu

Spatially dependent transfer functions for web span lateral dynamics which provide web lateral position and slope as outputs at any location in the web span are derived in this paper. The proposed approach overcomes one of the key limitations of the existing methods which provide web lateral position only on the rollers. The approach relies on taking the Laplace transform with respect to the temporal variable of both the web span lateral governing equation and the boundary conditions on the rollers, and solving the resulting equations. A general web span lateral transfer function, which is an explicit function of the spatial position along the span, is obtained first followed by its application to common guide configurations. The approach also significantly simplifies the consideration of shear (relevant to short spans), in addition to bending, which has been found to be difficult to handle in past studies. We first develop spatially dependent lateral transfer functions by considering only bending which is relevant to most web handling situations, and then add shear to the formulation and develop spatially dependent lateral transfer functions that include both bending and shear. Results from model simulations and pertinent discussions are provided. The spatially dependent transfer functions derived in this paper are a significant improvement over existing lateral transfer functions and provide mechanisms to analyze web lateral behavior within spans, study propagation of lateral disturbances, and aid in the development of closed-loop lateral control systems in emerging applications that require precise lateral positioning of the web.
[DOI: 10.1115/1.4040216]

1 Introduction

In Roll-to-Roll (R2R) manufacturing, flexible materials called webs are transported on rollers through processes (such as printing, coating, heat treatment, lamination, etc.). Studies in the literature have mostly focused on modeling and control of moving webs in the longitudinal or transport direction. In many applications, control of lateral web motion (motion perpendicular to the transport direction and in the plane of the web) has been mostly relegated to just keeping the web on rollers during transport. Increased use of R2R manufacturing in recent years on a variety of polymer materials under different processing conditions, in both conventional products and emerging products in flexible electronics, has led to additional requirements on the control of lateral motion of the web. For example, in R2R printing where multiple print cylinders are employed to sequentially print and register patterns on the web [1], there have been stringent requirements on minimizing print registration in both longitudinal and lateral directions.

There have been several studies on modeling the lateral behavior of moving webs. The first seminal work on the topic was reported by Shelton in his Ph.D. thesis in 1968 [2] and subsequently published in this journal [3,4]. Subsequent work in modeling and control of web lateral dynamics based on this treatment was reported in Refs. [5–9]. For the purpose of deriving the governing equations of the web lateral position on rollers, the moving web between two rollers is treated as a tensioned Euler–Bernoulli beam. For most web materials, the web mass between two rollers is negligible, i.e., the force due to acceleration of web mass is negligible when compared to web tension. Thus, the lateral motion of the web between two rollers is treated as the motion of a static beam; and the web between two rollers is treated as a tensioned beam. Four boundary conditions (web lateral position and slope on each roller) are utilized to solve the fourth-order partial differential equation describing the lateral motion of the web. A key observation/principle is utilized to setup two of the boundary conditions—a web approaching a roller aligns itself normal to the axis of rotation of the roller. This is also well known in the belt transport literature. This principle is utilized to setup two normal entry conditions: web lateral velocity and acceleration in terms of roller lateral velocity and acceleration, web entry angle at the roller, and angle of the roller. Based on this approach, transfer functions from the guide roller lateral position (input variable) to the web lateral position on the roller (controlled or output variable) are determined for various guide roller mechanisms, such as the end-pivoted guide, center-pivoted guide, offset pivot guide (OPG), remotely pivoted guide (RPG), etc. Figure 1 provides an illustration of a web span with upstream (entry) and downstream (exit) rollers and the definition of web wrap angle on a roller.

There are several limitations to the existing approach: (1) it provides a governing equation only for the lateral position behavior on the roller and not for any position within the span and (2) it does not the slope of the web which may contribute to the creation of web lateral oscillations and their propagation to downstream spans with web transport. Further, in the existing approach, the solution (lateral position) of the lateral governing equation is obtained by assuming constant downstream boundary conditions (on the downstream roller of the span); subsequently, the time derivative of the solution is used in the normal entry conditions to determine the transfer function for the lateral position on the roller. The purpose of the guide roller is to modify the downstream boundary conditions, and therefore, the assumption on the downstream boundary conditions is counter to the notion that the

[1]Corresponding author.

Contributed by the Dynamic Systems Division of ASME for publication in the Journal of Dynamic Systems, Measurement, and Control. Manuscript received September 11, 2017; final manuscript received May 2, 2018; published online June 18, 2018. Assoc. Editor: Mazen Farhood.

axis of rotation and translation of the guide roller is utilized to change the web boundary conditions on the roller. In this paper, we address these issues and derive spatially dependent lateral transfer functions that provide the web lateral position and slope at any point in the web span and not just on the roller.

Our approach relies on taking the Laplace transform of the web span lateral governing equation and the boundary conditions with respect to the temporal variable. We consider the web lateral position and slope on the upstream roller to the span as two boundary conditions and the two normal entry conditions (for lateral velocity and lateral acceleration) on the downstream roller as the other two boundary conditions. The idea of incorporating the normal entry conditions as boundary conditions has been considered in Ref. [6] where the normal entry conditions are applied to a system modeled using a dynamic beam equation; a two-dimensional Laplace transform (for both spatial and temporal variables) was applied to the dynamic beam equation which provides a solution to the beam equation in the frequency domain. Due to the complexity of determining the inverse Laplace transform of the resulting solution, the frequency domain solution was ignored and the spatial derivatives in the beam model were discretized using a finite difference method to obtain a set of ordinary differential equations for web lateral response on the roller; a two-span system example was used to illustrate the procedure. In our approach, we employ the Laplace transform in the temporal variable not only for the beam governing equation, but also for the two boundary conditions on the upstream roller and the two normal entry conditions on the downstream roller. This allows us to solve the resulting equations and obtain spatially dependent lateral transfer functions. The application of the Laplace transforms in the temporal variable for distributed parameter systems is discussed in Ref. [10].

The contributions of the paper are summarized in the following. First, we derive spatially dependent transfer functions for web lateral dynamics where the output can be any point spatially along the span. Further, we also derive transfer functions for web slope as the output at any point in the span. This is important as one can derive controllers to regulate lateral position at any point in the span, and investigate strategies that minimize propagation of lateral position and slope errors into the downstream spans. Second, the derived spatially dependent transfer functions can be applied to any guide configuration and specific transfer functions for those guiding situations can be determined. Third, we incorporate shear into the formulation by modifying the lateral governing equation and normal entry conditions appropriately. We use the same approach as before to derive the spatially dependent lateral transfer functions that include both bending and shear. The pure bending case is relevant to long spans, i.e., spans with large web span length to web width ratio, whereas the effect of shear is more prevalent in short spans. Further, since the proposed approach allows us to obtain not only position but also slope at any location in the span, one need not use multiple sensors to determine the position and slope of the web within the span as is done in some existing studies.

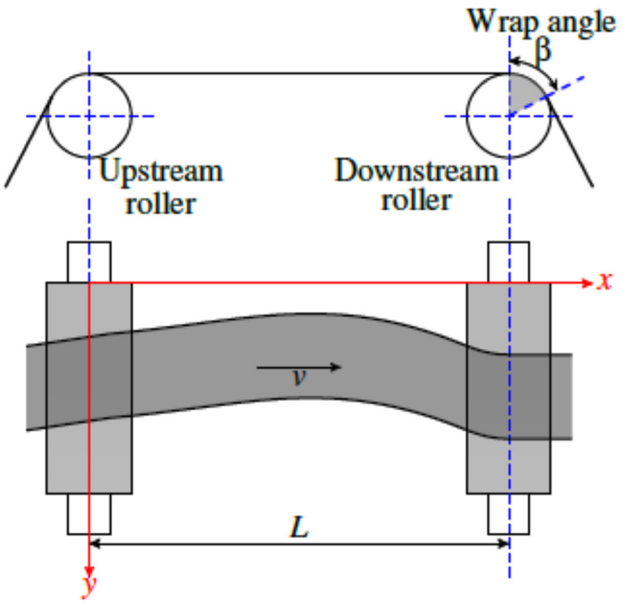

Fig. 1 Web span consider for modeling

The rest of the paper is organized as follows: In Sec. 2, we provide a discussion of the existing approach and its assumptions and limitations. The spatially dependent transfer functions for the pure bending case are derived, and application of the spatially dependent lateral transfer function to specific guiding configurations is given in Sec. 3. Inclusion of shear into the lateral governing equation and modification of the normal entry conditions are discussed in Sec. 4; spatially dependent lateral transfer functions for lateral position and slope for combined bending and shear are also given in this section. Numerical simulations for different guiding configurations are discussed in Sec. 5. Concluding remarks and future work are provided in Sec. 6.

2 Existing Approach and Assumptions

The governing equation for the web lateral dynamics is given by Shelton [2]

$$EI\frac{\partial^4 y(x,t)}{\partial x^4} - T\frac{\partial^2 y(x,t)}{\partial x^2} = 0 \tag{1}$$

The above-mentioned equation is similar to treating the web as a tensioned Euler–Bernoulli static beam, i.e., the web between two rollers is treated as a static beam by assuming the web mass to be negligible. The general solution to this equation is given by

$$y(x,t) = C_1\sinh(Kx) + C_2\cosh(Kx) + C_3x + C_4 \tag{2}$$

where $K^2 = T/EI$. Four boundary conditions are utilized to obtain the coefficients in the solution (2). These are typically assumed to be the lateral position (y) and slope ($\partial y/\partial x$) at the two ends of the web span, which are assumed to be known and given by

$$\begin{aligned} y(0,t) &= y_0(t), \quad \frac{\partial y}{\partial x}(x,t)|_{x=0} = \theta_{w0}(t), \\ y(L,t) &= y_L(t), \quad \frac{\partial y}{\partial x}(x,t)|_{x=L} = \theta_{wL}(t) \end{aligned} \tag{3}$$

where the subscripts 0 and L are utilized to denote variables at the entry and exit rollers, respectively, of the web span under consideration. Note that these boundary conditions imply that both ends of the tensioned beam (web span) are free.

The effect of the rollers on the lateral position of the web is modeled as follows. Friction between the roller and web surfaces is assumed to be adequate such that the web surface immediately aligns perpendicular to the roller axis of rotation when it makes contact with the roller. This observation is well known among researchers in both the web handling and the belt transport communities; this is typically referred to as the "normal entry rule" in the web handling community. Figure 2 provides a line sketch showing the relationship between the web slope and the lateral displacement of the roller. The web lateral velocities and accelerations are given by Shelton [2]

$$\frac{\partial y_L(t)}{\partial t} = v\left(\theta_L(t) - \frac{\partial y(x,t)}{\partial x}\bigg|_{x=L}\right) + \frac{\partial z_L(t)}{\partial t} \tag{4}$$

$$\frac{\partial^2 y_L(t)}{\partial t^2} = v^2\frac{\partial^2 y(x,t)}{\partial x^2}\bigg|_{x=L} + \frac{\partial^2 z_L(t)}{\partial t^2} \tag{5}$$

Note that the normal entry rule is used as a mechanism by which a guide roller can control the lateral position of the web via the rotation and translation of the guide roller by an actuating mechanism.

The lateral web position response on a roller is analyzed for two separate conditions: for fixed rollers ($z_L = 0$, $\theta_L = 0$) and steering or guide rollers ($z_L \neq 0$, $\theta_L \neq 0$). The responses are combined by assuming that the principle of superposition applies to this situation. The governing equation for the evolution of the lateral position for the two conditions is obtained as follows. First, the second partial derivative of Eq. (2) with respect to x is substituted into Eq. (5). The resulting equation contains the web angle, θ_{wL}, which is replaced by the slope term from the entry rule given by Eq. (4). Taking the Laplace transform of the resulting equation with respect to time results in the following lateral response at the downstream roller due to various inputs [7]:

$$y_L(s) = \frac{-\frac{f_3(KL)}{\tau}s + \frac{f_1(KL)}{\tau^2}}{D(S)} y_0(s) + \frac{\frac{vf_3(KL)}{\tau}}{D(s)}\theta_0(s) + \frac{\frac{vf_2(KL)}{\tau}}{D(s)}\theta_L(s) + \frac{\frac{f_3(KL)}{\tau}s}{D(s)} z_0(s) + \frac{s^2 + \frac{f_2(KL)}{\tau}s}{D(s)} z_L(s) \tag{6}$$

where $\tau = L/v$, $D(s) = s^2 + (f_2(KL)/\tau)s + (f_1(KL)/\tau^2)$

$$\Delta_f = KL\sinh(KL) + 2(1 - \cosh(KL))],$$
$$f_1(KL) = (KL)^2(\cosh(KL) - 1)/\Delta_f$$
$$f_2(KL) = KL[KL(\cosh(KL) - \sinh(KL))]/\Delta_f,$$
$$f_3(KL) = KL[\sinh(KL) - KL]/\Delta_f$$

Remark 2.1. This existing approach has several drawbacks: (1) it provides the evolution of the lateral position only on the roller; it does not provide lateral web position within the span. (2) Although lateral position at the downstream roller is of interest, this is assumed as a known boundary condition in the development. (3) The normal entry conditions are used in an indirect manner in the sense that the knowledge of the lateral position and slope on the downstream roller are assumed to be known (resulting in the response at a specific location) and then these are applied to the resulting solution to fit the normal entry conditions.

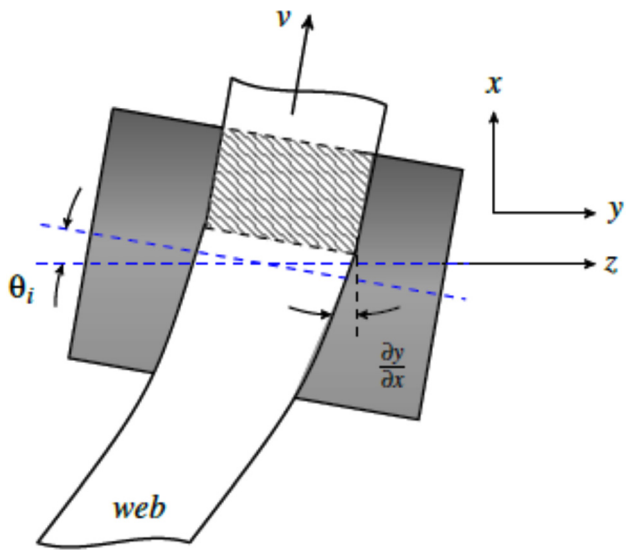

Fig. 2 Web behavior at roller entry (normal entry condition)

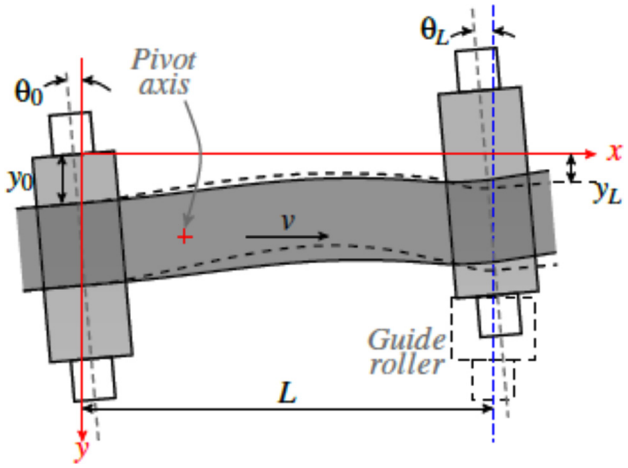

Fig. 3 Web span with RPG

3 Spatially Dependent Transfer Functions

In the existing approach (summarized in Sec. 2), the effect of the boundary conditions on web lateral behavior within the free span is not clear. The "normal entry rule" is applied to introduce a dynamical behavior on the roller and to obtain a relationship between the lateral web position on the guide roller and the control action (guide roller motion). In this work, instead of assuming the downstream boundary conditions for lateral position and slope (at $x = L$) (whose evolution is of interest), the two normal entry conditions are employed as downstream boundary conditions. This allows for directly incorporating the effect of the roller into the solution of the governing equation. Further, this also allows for directly coupling the dynamic effects of the rollers with the span lateral dynamics.

We define a free span as the length of material between two rollers that is not wrapped on the rollers. For the upstream roller, we establish the boundary conditions for the span at the exit of the region of wrap of the upstream roller. Due to the application of

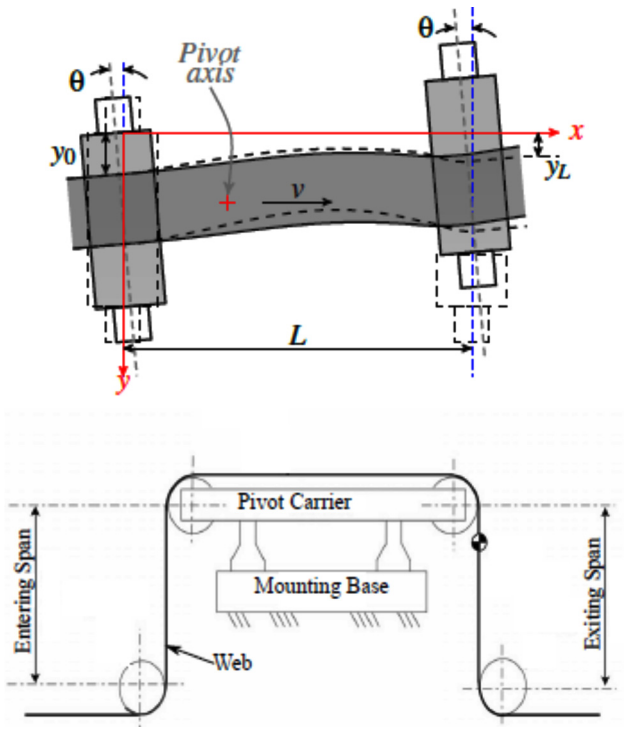

Fig. 4 Web span with OPG

the normal entry rule to the upstream roller, which stipulates that the web aligns perpendicular to the roller at contact, the web leaves this roller perpendicularly. Then, the upstream roller angle becomes a boundary condition for web slope. In the region of wrap of the upstream roller, the lateral displacement remains the same throughout, which is taken as the second boundary condition at the beginning of the span.

To solve the governing equation, we apply the Laplace transform in the temporal variable for both the governing equation and the boundary conditions. The governing equations given by Eq. (1) and the boundary conditions are rewritten compactly as

$$y(0,t)=y_0(t);\quad \frac{\partial y(0,t)}{\partial x}=\theta_0(t);\quad \frac{\partial y(L,t)}{\partial x}=\theta_L(t)+\frac{1}{v}\frac{\partial z(t)}{\partial t}-\frac{1}{v}\frac{\partial y(L,t)}{\partial t};\quad \frac{\partial^2 y(L,t)}{\partial x^2}=\frac{1}{v^2}\left(\frac{\partial^2 y(L,t)}{\partial t^2}-\frac{\partial^2 z(t)}{\partial t^2}\right) \tag{7}$$

The conditions at $x=0$ represent web lateral position and web slope at the entry of the span (exit of the region of wrap of the upstream roller); the slope is the same as the upstream roller angle $\theta_0(t)$, due to the interpretation of the entry rule for the web on that roller. The other two conditions at $x=L$ are the normal entry rules at the entry of the region of wrap for the downstream roller. We will apply the following Laplace transform for the time variable:

$$\mathcal{L}\{f(x,t)\}=\hat{f}(x,s)=\int_0^\infty e^{-st}f(x,t)dt \tag{8}$$

to the web governing Eq. (1) and the boundary conditions (7) to obtain

$$\frac{\partial^4\hat{y}(x,s)}{\partial x^4}-K^2\frac{\partial^2\hat{y}(x,s)}{\partial x^2}=0 \tag{9}$$

and

$$\hat{y}(0,s)=\hat{y}_0(s);\quad \frac{\partial\hat{y}(0,s)}{\partial x}=\hat{\theta}_0(s);\quad \frac{\partial\hat{y}(L,s)}{\partial x}=\hat{\theta}_L(s)+\frac{s}{v}\hat{z}_L(s)-\frac{s}{v}\hat{y}_L(s);\quad \frac{\partial^2\hat{y}(L,s)}{\partial x^2}=\frac{s^2}{v^2}\hat{y}_L(s)-\frac{s^2}{v^2}\hat{z}_L(s) \tag{10}$$

The general solution of Eq. (9) is given by

$$\hat{y}(x,s)=C_1(s)\sinh(Kx)+C_2(s)\cosh(Kx)+C_3(s)x+C_4(s) \tag{11}$$

Note that the coefficients C_i are functions of the variable s. Substituting the boundary conditions into Eq. (11) results in the following solution:

$$\hat{y}(x,s)=-\left(\frac{s^2}{v^2}g_2(x)+\frac{s}{v}g_1(x)\right)\hat{y}_L(s)+\left(\frac{s^2}{v^2}g_2(x)+\frac{s}{v}g_1(x)\right)\hat{z}_L(s)+\hat{y}_0(s)+g_1(x)\hat{\theta}_L(s)+(x-g_1(x))\hat{\theta}_0(s) \tag{12}$$

where we have used the notation $\hat{y}_L(s)=\hat{y}(L,s)$ and

$$\begin{aligned} g_1(x)&=\frac{\sinh(KL)[\cosh(Kx)-1]-\cosh(KL)[\sinh(Kx)-Kx]}{K[\cosh(KL)-1]}\\ g_2(x)&=\frac{[\cosh(KL)-1][\cosh(Kx)-1]-\sinh(KL)[\sinh(Kx)-Kx]}{K^2[\cosh(KL)-1]}\end{aligned} \tag{13}$$

Note that the slope and moment at any location inside the span are given by

$$\frac{\partial\hat{y}}{\partial x}(x,s)=-\left(\frac{s^2}{v^2}g_{2x}(x)+\frac{s}{v}g_{1x}(x)\right)\hat{y}_L(s)+\left(\frac{s^2}{v^2}g_{2x}(x)+\frac{s}{v}g_{1x}(x)\right)\hat{z}_L(s)+g_{1x}(x)\hat{\theta}_L(s)+(1-g_{1x}(x))\hat{\theta}_0(s) \tag{14}$$

$$\frac{\partial^2\hat{y}}{\partial x^2}(x,s)=-\left(\frac{s^2}{v^2}g_{2xx}(x)+\frac{s}{v}g_{1xx}(x)\right)\hat{y}_L(s)+\left(\frac{s^2}{v^2}g_{2xx}(x)+\frac{s}{v}g_{1xx}(x)\right)\hat{z}_L(s)+g_{1xx}(x)\hat{\theta}_L(s)-g_{1xx}(x)\hat{\theta}_0(s) \tag{15}$$

where $g_{lx}(x)$ is the first partial derivative of $g_l(x)$ with respect to x ($l=1,2$) and $g_{lxx}(x)$ is the second partial derivative. Note that $g_{1x}(L)=1$, $g_{2x}(L)=0$, $g_{1xx}(L)=0$, $g_{2xx}(L)=-1$.

Define $D_b(s)=s^2+vg_1(L)/g_2(L)s+v^2/g_2(L)$. When $x=L$, Eq. (12) can be simplified to

$$\hat{y}_L(s)=\frac{s^2+v\dfrac{g_1(L)}{g_2(L)}s}{D_b(s)}\hat{z}_L(s)+\frac{\dfrac{g_1(L)}{g_2(L)}v^2}{D_b(s)}\hat{\theta}_L(s)+\frac{\dfrac{L-g_1(L)}{g_2(L)}v^2}{D_b(s)}\hat{\theta}_0(s)+\frac{\dfrac{1}{g_2(L)}v^2}{D_b(s)}\hat{y}_0(s) \tag{16}$$

Substituting Eq. (16) into Eq. (12) and simplifying we obtain

$$\hat{y}(x,s)=\frac{P_4(x,s)}{D_b(s)}\hat{z}_L(s)+\frac{P_3(x,s)}{D_b(s)}\hat{\theta}_L(s)+\frac{P_1(x,s)}{D_b(s)}\hat{\theta}_0(s)+\frac{P_2(x,s)}{D_b(s)}\hat{y}_0(s) \tag{17}$$

Table 1 Lateral response for various roller configurations

Setup	Conditions	Equation
Downstream fixed roller	$\hat{\theta}_L(s)=0,\ \hat{z}_L(s)=0$	$\hat{y}(x,s)=\frac{P_1(x,s)}{D_b(s)}\hat{\theta}_0(s)+\frac{P_2(x,s)}{D_b(s)}\hat{y}_0(s)$
Pure displacement	$\hat{\theta}_L(s)=0$	$\hat{y}(x,s)=\frac{P_1(x,s)}{D_b(s)}\hat{\theta}_0(s)+\frac{P_2(x,s)}{D_b(s)}\hat{y}_0(s)+\frac{P_4(x,s)}{D_b(s)}\hat{z}_L(s)$
Pure rotation	$\hat{z}_L(s)=0$	$\hat{y}(x,s)=\frac{P_1(x,s)}{D_b(s)}\hat{\theta}_0(s)+\frac{P_2(x,s)}{D_b(s)}\hat{y}_0(s)+\frac{P_3(x,s)}{D_b(s)}\hat{\theta}_L(s)$
RPG (see Fig. 3)	$\hat{z}_L(s)=X_1\hat{\theta}_L(s)$	$\hat{y}(x,s)=\frac{P_1(x,s)}{D_b(s)}\hat{\theta}_0(s)+\frac{P_2(x,s)}{D_b(s)}\hat{y}_0(s)+\frac{P_5(x,s)}{D_b(s)}\hat{\theta}_L(s)$ where $P_5(x,s)=P_3(x,s)+X_1P_4(x,s)$
OPG (see Fig. 4)	$\hat{\theta}_0(s)=\hat{\theta}_L(s)=\hat{\theta}(s)$	$\hat{y}(x,s)=\frac{P_6(x,s)}{D_b(s)}\hat{\theta}(s)+\frac{P_2(x,s)}{D_b(s)}\hat{y}_0(s)$ where $P_6(x,s)=P_1(x,s)+P_3(x,s)+X_1P_4(x,s)$

where

$$
\begin{aligned}
P_1(x,s)&=\frac{1}{g_2(L)}\left[\left((x-g_1(x))g_2(L)-\big(L-g_1(L)\big)g_2(x)\right)s^2\right.\\
&\quad\left.+v\big(xg_1(L)-Lg_1(x)\big)\right)s+(x-g_1(x))v^2\Big]\\
P_2(x,s)&=\frac{1}{g_2(L)}\Big[\big(g_2(L)-g_2(x)\big)s^2+v\big(g_1(L)-g_1(x)\big)s+v^2\Big]\\
P_3(x,s)&=\frac{1}{g_2(L)}\Big[\big(g_1(x)g_2(L)-g_1(L)g_2(x)\big)s^2+v^2g_1(x)\Big]\\
P_4(x,s)&=\frac{1}{g_2(L)}\big[g_2(x)s^2+vg_1(x)s\big]
\end{aligned}
\tag{18}
$$

Equation (17) provides the spatially dependent Laplace transform of the lateral position in terms of various inputs and their associated transfer functions. Further, one can obtain transfer functions for slope and moment at any location along the web span by substituting Eq. (16) in Eqs. (14) and (15).

3.1 Comparison With Existing Transfer Functions. Since the approach in this work provides transfer functions from control and disturbance inputs to lateral position output at any location in the span, we can compare it with the general transfer functions given in Ref. [7] when $x=L$. Note that at $x=L$, we can write the following relations:

$$
\begin{aligned}
g_1(L)&=\frac{KL\cosh(KL)-\sinh(KL)}{K[\cosh(KL)-1]}\\
g_2(L)&=\frac{KL\sinh(KL)+2[1-\cosh(KL)]}{K^2[\cosh(KL)-1]}\quad\left(=\frac{L^2}{f_1(KL)}\right)\\
\frac{L-g_1(L)}{g_2(L)}&=\frac{K\sinh(KL)-KL}{KL\sinh(KL)+2[1-\cosh(KL)]}\quad\left(=\frac{f_3(KL)}{L}\right)\\
\frac{g_1(L)}{g_2(L)}&=\frac{K[KL\cosh(KL)-\sinh(KL)]}{KL\sinh(KL)+2[1-\cosh(KL)]}\quad\left(=\frac{f_2(KL)}{L}\right)
\end{aligned}
\tag{19}
$$

Substitution of these relations in Eq. (16) results in the web lateral position response on the roller at $x=L$

$$
\begin{aligned}
y_L(s)&=\frac{s^2+\dfrac{f_2(KL)}{\tau}s}{D(s)}\hat{z}_L(s)+\frac{\dfrac{vf_2(KL)}{\tau}}{D(s)}\hat{\theta}_L(s)+\frac{\dfrac{f_1(KL)}{\tau^2}}{D(s)}\hat{y}_0(s)\\
&\quad+\frac{\dfrac{vf_3(KL)}{\tau}}{D(s)}\hat{\theta}_0(s)
\end{aligned}
\tag{20}
$$

This differs slightly from Eq. (6) because in the existing approach the free span definition included the region of wrap also, and the entry rule was applied to the upstream roller in the following manner:

$$
\hat{y}(0,s)=\hat{y}_0(s);\quad \frac{\partial\hat{y}}{\partial x}(0,s)=\frac{\partial\hat{y}}{\partial x}|_{x=0,s}=\hat{\theta}_{w0}(s)=-\frac{s}{v}\hat{y}_0(s)
\tag{21}
$$

However, in our approach, the free span does not include the region of wrap in either the upstream or downstream rollers; the interpretation of the normal entry rule is that the web will acquire the roller angle and keep it for the entire region of wrap; due to this the first term in the numerator of $y_0(s)$ and $z_0(s)$ cancel each other. The following remarks provide some observations based on the results of this section.

Remark 3.1. By employing normal entry conditions on the downstream roller of the span as the boundary conditions, we incorporated the effect of web/roller contact into the solution of the governing equation. The proposed method allows us to directly obtain higher order spatial partial derivatives of the lateral response and thus can be used for obtaining web slope, moment, shear force, etc. The method also further opens up the opportunity to develop controllers for processes which require control of lateral position within the span.

Remark 3.2. The proposed method can be extended to include shear by establishing appropriate boundary conditions. The inclusion of shear modifies the boundary condition for the lateral acceleration and introduces an additional pole and zero in the lateral transfer functions. This is discussed later in Sec. 4.

Equation (17) is the general expression for spatially dependent web lateral position and further simplification of this equation can be achieved by considering the specific roller configuration corresponding to a given situation. This is shown in Table 1 for the most common situations.

The following remarks provide a perspective for each item in Table 1. With a fixed downstream roller, the response depends only on the perturbations ($\hat{y}_0(s)$, $\hat{\theta}_0(s)$) at the entry of the span. To regulate web lateral position, one has to control both position and slope; much of the existing work has focused only on regulating the lateral position at the exit of the guide without accounting for the roller angle. Note that in most guide installations, the plane of the guiding span and the span downstream of it are perpendicular to each other; if this is not the case, then the roller angle will affect downstream lateral position. We will illustrate this effect in subsequent model simulations. Note that the second and third items in Table 1 correspond to a pure displacement guide roller (with $\hat{z}_L(s)$ as the input) and pure rotation guide roller (with $\hat{\theta}_L(s)$ as the input); these could be used for terminal guiding on unwind and rewind rollers. The last two items correspond to two commonly used intermediate guides.

4 Consideration of Shear

The main assumption in the development of the tensioned beam model (Euler–Bernoulli beam) is that under loading, the cross-sectional area of the beam remains perpendicular to the neutral axis. However, for beams with smaller length to width ratio, this assumption may not hold, as the effect of shear is significant. This is also true for short web spans as discussed in Refs. [2], [5], and [11]. In this section we develop spatially dependent transfer functions by adding shear to the bending case considered in Sec. 3. The slope due to shear force may be expressed as

$$\frac{\partial y_s(x,t)}{\partial x} = \frac{nN}{AG} \tag{22}$$

where n is the correction factor and is equal to 1.2 for webs with rectangular cross-sectional area, A is the web cross section area, and G is the shear modulus. We will use subscript t to refer to the total deflection due to combined bending and shear and subscripts b and s, respectively, for pure bending and pure shear. The tensioned beam governing equation that includes shear may be obtained by using the force equilibrium in the lateral direction. A free-body diagram of the web is provided in Fig. 5(*a*). The shear force may be expressed as

$$N(x) = T\left(\theta_L - \frac{\partial y_t(x,t)}{\partial x}\right) + N(L) \tag{23}$$

Taking two consecutive partial derivatives with respect to x of Eqs. (22) and (23) and combining the resulting two equations result in the following:

$$\frac{\partial^3 y_s(x,t)}{\partial x^3} = -\frac{nT}{AG}\frac{\partial^3 y_t(x,t)}{\partial x^3} \tag{24}$$

Further, the shear force due to bending is given by

$$N(x) = -EI\frac{\partial^3 y_b(x,t)}{\partial x^3} \tag{25}$$

Figure 5(*b*) provides a visualization of the bending and shear angles, and the resulting slope of the web; note that $\partial y_t/\partial x = \partial y_b/\partial x + \partial y_s/\partial x$. Using the angle relationship, one can write

$$N(x) = -EI\frac{\partial^3 y_t(x,t)}{\partial x^3}\left[1 + \frac{nT}{AG}\right] \tag{26}$$

Taking the partial derivative with respect to x and employing $\partial N(x)/\partial x = -T\partial^2 y_t(x,t)/\partial x^2$ (obtained from Eq. (23)), one can establish the following governing equation for the web that includes both bending and shear:

$$\frac{\partial^4 y_t(x,t)}{\partial x^4} - K_e^2\frac{\partial^2 y_t(x,t)}{\partial x^2} = 0 \tag{27}$$

where $K_e^2 = T/(EI[1 + nT/AG])$. Equation (27) is similar to the pure bending case, except that K is replaced by K_e which is related to K as $K_e^2 = K^2/[1 + nT/AG]$. Note that if shear is not considered, we can set $n = 0$ to obtain $K_e = K$.

The inclusion of shear changes the normal entry condition related to the acceleration. The two boundary conditions corresponding to the position and slope on the upstream roller do not change except for using the total response, y_t; these are given by

$$y(0,t) = y_0(t), \quad \frac{\partial y_t(0,t)}{\partial x} = \theta_0(t) \tag{28}$$

The third boundary condition for slope at the downstream roller does not change also because shear is included in the total slope and is given by

$$\frac{\partial y_t(L,t)}{\partial x} = \theta_L(t) + \frac{1}{v}\frac{\partial z_L(t)}{\partial t} - \frac{1}{v}\frac{\partial y_t(L,t)}{\partial t} \tag{29}$$

To determine the fourth boundary condition, we first have to consider the following relationship for web rotational velocity at the downstream roller [11]:

$$\frac{\partial \theta_L(t)}{\partial t} = \frac{\partial^2 y_b(L,t)}{\partial t \partial x} + v\frac{\partial^2 y_b(L,t)}{\partial x^2} \tag{30}$$

Taking the time derivative of Eq. (29), we obtain

$$\frac{\partial^2 y_t(L,t)}{\partial t^2} = v\frac{\partial \theta_L(t)}{\partial t} - v\frac{\partial}{\partial t}\frac{\partial y_t(L,t)}{\partial x} + \frac{\partial^2 z_L(t)}{\partial t^2} \tag{31}$$

Then, using $\partial y_b/\partial x = \partial y_t/\partial x - \partial y_s/\partial x$ in Eq. (30) and substituting the result into Eq. (31), we obtain the fourth condition boundary condition as

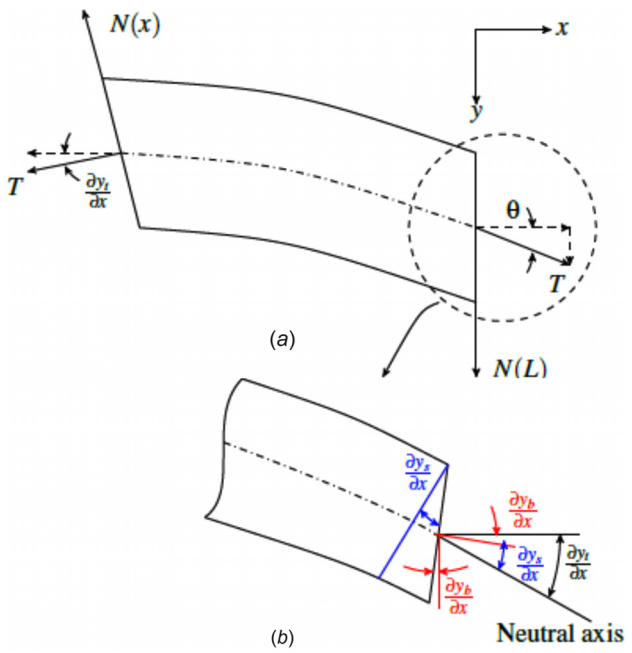

Fig. 5 Effect of shear: (*a*) free body forces and (*b*) slope

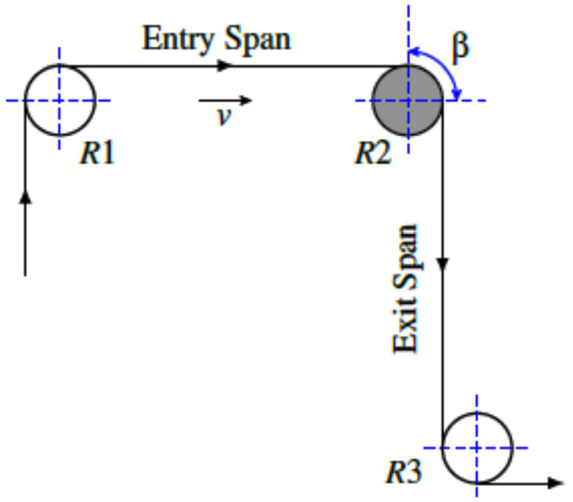

Fig. 6 Two-span, three-roller system

$$\frac{\partial^2 y_t(L,t)}{\partial x^2} = \frac{1}{v^2}\left(\frac{\partial^2 y_t(L,t)}{\partial t^2} - \frac{\partial^2 z_L(t)}{\partial t^2}\right) + \frac{1}{v}\left(\frac{\partial}{\partial t}\frac{\partial y_s(L,t)}{\partial x} + v\frac{\partial^2 y_s(L,t)}{\partial x^2}\right) \tag{32}$$

The previously-mentioned boundary condition for lateral acceleration is in terms of the shear angle. A relationship for shear angle $(\partial y_s/\partial x)$ in terms of y_t would aid in determining the coefficients of the general solution of the governing equation. To determine such a relationship, the shear force expressed by Eq. (26) is used in Eq. (22). This results in

$$\frac{\partial y_s(x,t)}{\partial x} = \frac{n}{AG}\left(-EI\frac{\partial^3 y_t(x,t)}{\partial x^3}\left[1 + \frac{nT}{AG}\right]\right) \tag{33}$$

A Hamiltonian method is used for finding such an expression in Ref. [12]. Now, using the definition of K_e^2, Eq. (33) may be written as

$$\frac{\partial y_s(x,t)}{\partial x} = -\frac{nT}{AGK_e^2}\frac{\partial^3 y_t(x,t)}{\partial x^3} \tag{34}$$

Thus, the fourth boundary condition for lateral acceleration at the downstream roller may be written as

$$\frac{\partial^2 y_t(L,t)}{\partial x^2} = \frac{1}{v^2}\left(\frac{\partial^2 y_t(L,t)}{\partial x^2} - \frac{\partial^2 z_L(t)}{\partial x^2}\right) - \frac{nT}{vAGK_e^2}\left(\frac{\partial}{\partial t}\frac{\partial^3 y_t(L,t)}{\partial x^3} + v\frac{\partial^4 y_t(L,t)}{\partial x^4}\right) \tag{35}$$

Now, the governing equation and the boundary conditions are in terms of the total deflection. Applying the Laplace transform as defined in Eq. (8) to Eq. (27) and the modified boundary conditions that include shear, we obtain

$$\frac{\partial^4 \hat{y}_t(x,s)}{\partial x^4} - K_e^2\frac{\partial^2 \hat{y}_t(x,s)}{\partial x^2} = 0 \tag{36}$$

and

$$\begin{gathered}\hat{y}_t(0,s) = \hat{y}_0(s), \quad \frac{\partial \hat{y}_t(0,s)}{\partial x} = \hat{\theta}_0(s), \quad \frac{\partial \hat{y}_t(L,s)}{\partial x} = \hat{\theta}_L(s) + \frac{s}{v}\hat{z}_L(s) - \frac{s}{v}\hat{y}_t(L,s) \\ \frac{\partial^2 \hat{y}_t(L,s)}{\partial x^2} = \frac{s^2}{v^2}\left(\hat{y}_t(L,s) - \hat{z}(s)\right) - \frac{nTs}{vAGK_e^2}\frac{\partial^3 \hat{y}_t(L,s)}{\partial x^3} - \frac{nT}{AGK_e^2}\frac{\partial^4 \hat{y}_t(L,s)}{\partial x^4}\end{gathered} \tag{37}$$

The general solution of Eq. (36) is

$$\hat{y}_t(x,s) = C_{1e}(s)\sinh(K_e x) + C_{2e}(s)\cosh(K_e x) + C_{3e}(s)x + C_{4e}(s) \tag{38}$$

The coefficients $C_{ie}(s)$ are determined by using the boundary conditions (37). Let $g_{1e}(x)$ and $g_{2e}(x)$ denote the expressions for $g_1(x)$ and $g_2(x)$, respectively, by replacing K with K_e. Using the same approach as in the pure bending case, the total lateral response due to both bending and shear may be simplified to

$$\hat{y}(x,s) = \frac{\tilde{P}_1(x,s)}{D_{1s}(s)D_s(s)}\hat{\theta}_0(s) + \frac{\tilde{P}_2(x,s)}{D_s(s)}\hat{y}_0(s) + \frac{\tilde{P}_3(x,s)}{D_{1s}(s)D_s(s)}\hat{\theta}_L(s) + \frac{\tilde{P}_4(x,s)}{D_{1s}(s)D_s(s)}\hat{z}_L(s) \tag{39}$$

where

$$D_s(s) = s^2 + bs + c, \quad D_{1s}(s) = \gamma s + (1+a)v, \quad a = \frac{nT}{AG}, \quad \gamma = \frac{a\sinh(K_e L)}{K_e(\cosh(K_e L) - 1)}$$

$$b = \frac{v\left((1+a)g_{1e}(L) + \gamma\right)}{g_{2e}(L) - g_{3e}(L)}, \quad c = \frac{v^2(1+a)}{g_{2e}(L) - g_{3e}(L)}$$

$$g_{3e}(x) = a\frac{(\sinh(K_e L)(\sinh(K_e x) - K_e x) - \cosh(K_e L)(\cosh(K_e x) - 1))}{K_e^2(\cosh(KL) - 1)}$$

$$\begin{aligned}\tilde{P}_1(x,s) = \frac{1}{(g_{2e}(L) - g_{3e}(L))}\Big[&\left(g_{3e}(x)g_{2e}(L) - g_{2e}(x)g_{3e}(L) + \gamma\left(x\left(g_{2e}(L) - g_{3e}(L)\right) - L(g_{2e}(x) - g_{3e}(x))\right)\right)s^3 \\ &+ v\left((1+a)\left(\underbrace{(x - g_{1e}(x))g_{2e}(L) + \left(g_{1e}(L) - L\right)g_{2e}(x)}_{\text{bending}} + x\left(g_{1e}(L)\gamma - g_{3e}(L)\right) - L(\gamma g_{1e}(x) - g_{3e}(x))\right) + \gamma(x\gamma + g_{3e}(x))\right)s^2 \\ &+ v^2(1+a)\left(2x\gamma + g_{3e}(x) - \gamma g_{1e}(x) + (1+a)\underbrace{\left(xg_{1e}(L) - Lg_{1e}(x)\right)}_{\text{bending}}\right)s + (1+a)^2\underbrace{v^3(x - g_{1e}(x))}_{\text{bending}}\Big]\end{aligned} \tag{40}$$

$$\tilde{P}_2(x,s)=\frac{1}{\left(g_{2e}(L)-g_{3e}(L)\right)}\left[\left(\underbrace{g_{2e}(L)-g_{2e}(x)}_{\text{bending}}-g_{3e}(L)+g_{3e}(x)\right)s^2+v\left(\gamma+(1+a)\left(\underbrace{g_{1e}(L)-g_{1e}(x)}_{\text{bending}}\right)\right)s\quad+\underbrace{v^2}_{\text{bending}}(1+a)\right] \tag{41}$$

$$\tilde{P}_3(x,s)=\frac{1}{\left(g_{2e}(L)-g_{3e}(L)\right)}\left[\left(g_{2e}(x)g_{3e}(L)-g_{3e}(x)g_{2e}(L)\right)s^3+v\left((1+a)\left(\underbrace{g_{2e}(L)g_{1e}(x)-g_{1e}(L)g_{2e}(x)}_{\text{bending}}\right)-\gamma g_{3e}(x)\right)s^2\right.$$
$$\left.+v^2(1+a)(\gamma g_{1e}(x)-g_{3e}(x))s\quad+(1+a)^2\underbrace{v^3g_{1e}(x)}_{\text{bending}}\right] \tag{42}$$

$$\tilde{P}_4(x,s)=\frac{1}{\left(g_{2e}(L)-g_{3e}(L)\right)}\left[\gamma(g_{2e}(x)-g_{3e}(x))s^3+v(1+a)\left(\underbrace{g_{2e}(x)}_{\text{bending}}-g_{3e}(x)+\gamma g_{1e}(x)\right)s^2+(1+a)^2\underbrace{v^2g_{1e}(x)}_{\text{bending}}s\right] \tag{43}$$

Table 2 Parameter values used in numerical simulations [7]

Definition	Symbol	Value	Units
Entry span length	L	3.2808 (1)	ft (m)
Exit span length	L	3.806 (1.16)	ft (m)
Integral gain	k_i	10	
Pivoting distance for OPG	X_1	3.52808 (1)	ft (m)
Pivoting distance for RPG	X_1	2.5833 (0.7874)	ft (m)
Proportional gain	k_p	90	
Reference tension	T	10 (44.48)	lbf (N)
Shear modulus	G	0.154 (1.062×10^9)	Mpsi (Pa)
Transport speed	v	500 (2.54)	ft/min (m/s)
Web thickness	h	0.005 (0.127)	in (mm)
Web width	W	5.4 (137.16)	in (mm)
Wrap angle	β	1.553 (89)	rad (deg)
Young's modulus	E	0.40466 (2.76×10^9)	Mpsi (Pa)

In the previously-mentioned definitions for $\tilde{P}_j, j=1:4$, terms that carry forward from the pure bending case are indicated. Inclusion of shear results in the additional terms in those definitions. Note that if shear is not considered, then $\gamma=0$, $g_{3e}(x)=0$, $g_{1e}(x)=g_1(x)$, and $g_{2e}(x)=g_2(x)$, and Eq. (39) reduces to Eq. (12)

Table 3 Simulation scenarios with single span

Figure	Parameters
Fig. 7	$\theta_0(t)=0.01\sin(3t)$ rad, $y_0=\theta_L=z_L=0$
Fig. 8	$\theta_L(t)=0.01\sin(3t)$ rad, $z_L(t)=X_1\theta_L(t)$, $y_0=\theta_0=0$

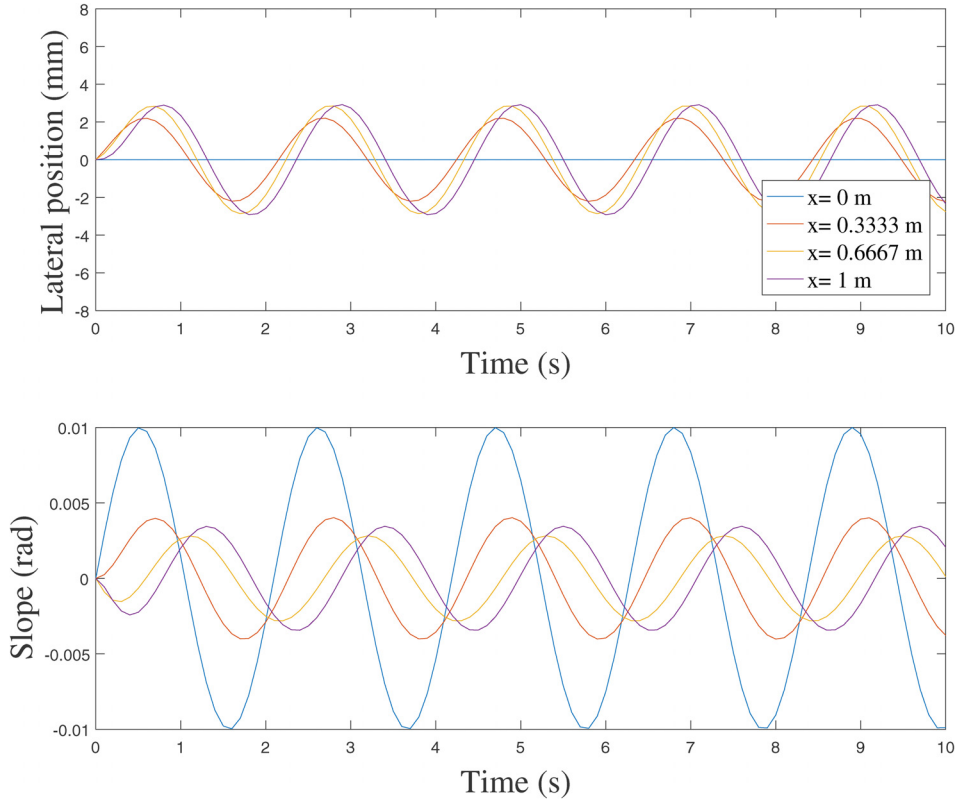

Fig. 7 Evolution of web lateral position and slope for 4 points along the span for a sinusoidal roller rotation of $\theta_0=0.01\sin(3t)$ of roller R1

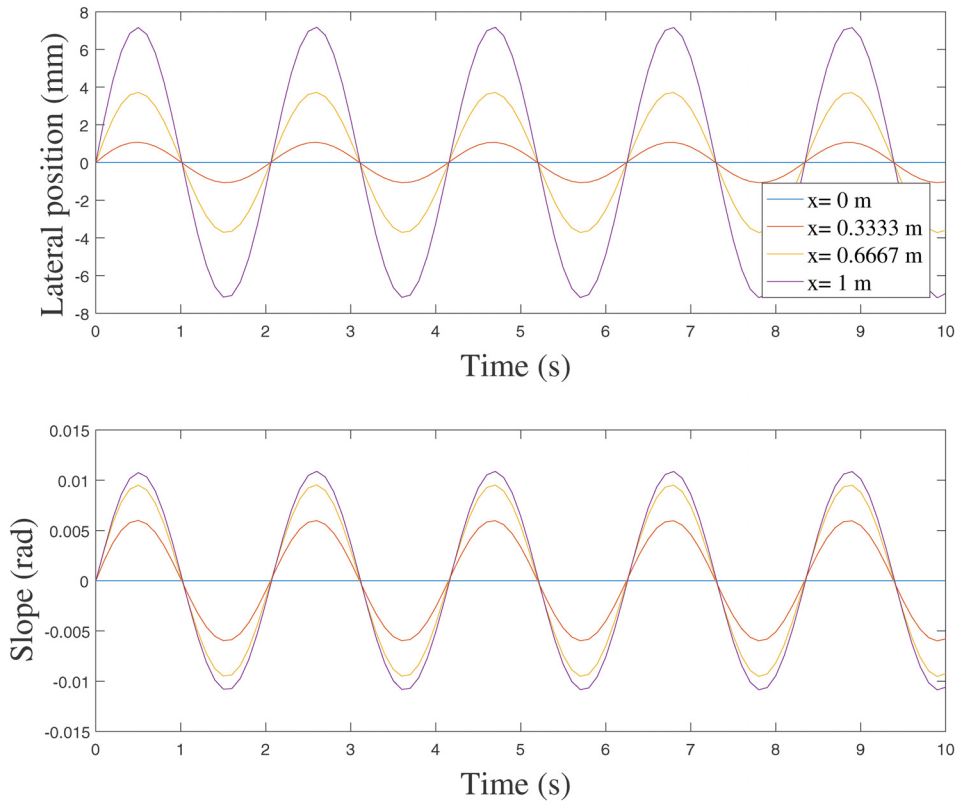

Fig. 8 Evolution of web lateral position and slope for 4 points along the span for a sinusoidal roller rotation of $\theta_L = 0.01 \sin(3t)$, $z_L = X_1\theta_L$ of roller R2

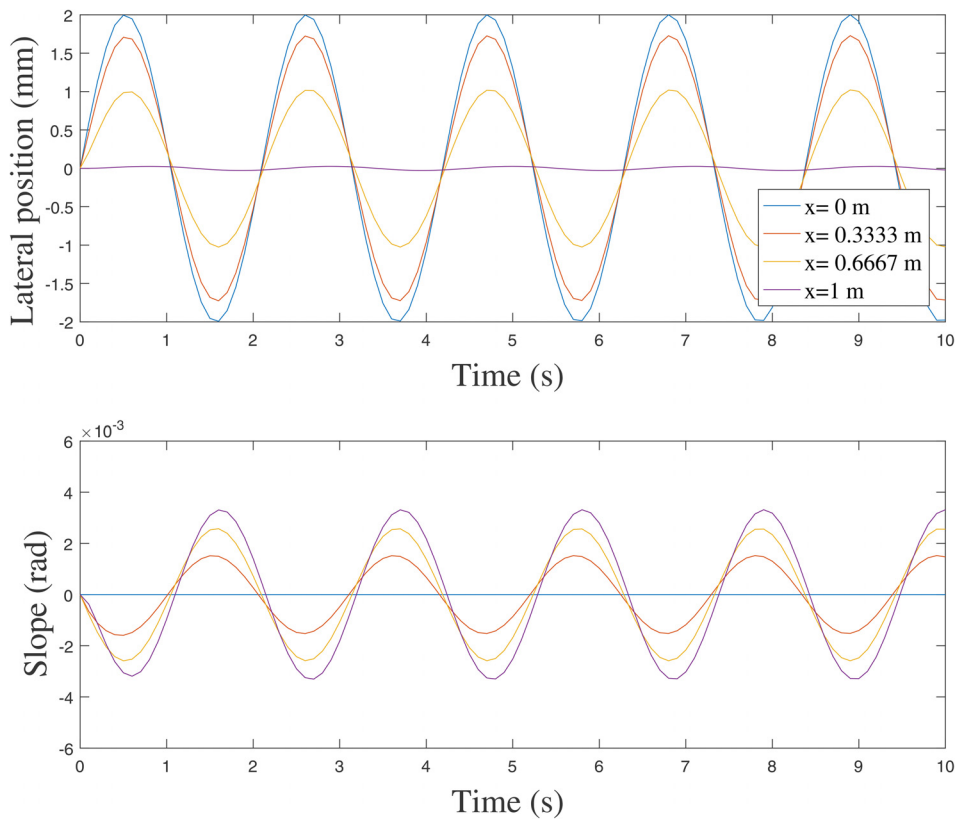

Fig. 9 Evolution of web lateral position and slope for 4 points along the entry span for a sinusoidal disturbance of $y_0 = 0.002 \sin(3t)$ on R1, with proportional–integral (PI) control of the RPG

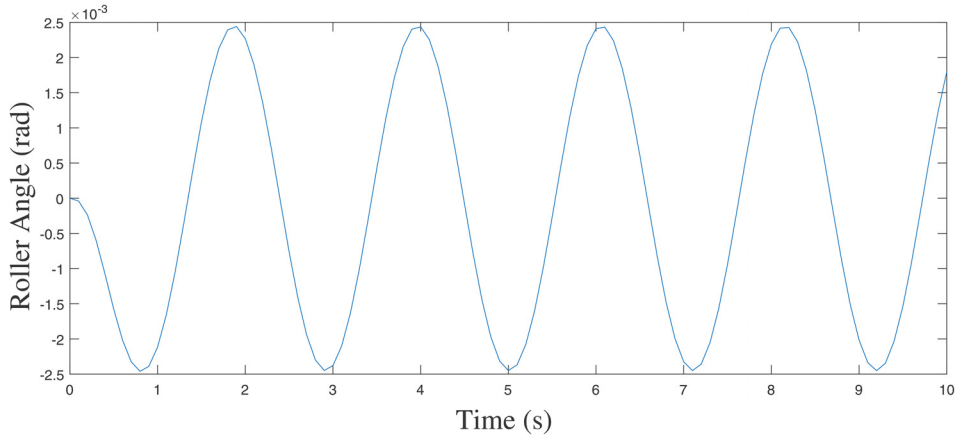

Fig. 10 Evolution of guide roller rotation ($\theta_L(t)$) with PI control in the plane of the entry span

5 Numerical Simulations

Numerical simulations were conducted with the lateral transfer functions that include both bending and shear. A three-roller system shown in Fig. 6 is considered. The numerical values of the web and guide parameters used in the simulations are provided in Table 2 [7]. For the first set of numerical simulations, we consider the governing equation for the span between rollers R1 and R2 (entry span), and apply different disturbance scenarios provided in Table 3. Figure 7 provides the evolution of the lateral web position and slope in the entry span at four different locations. One can observe that the web slope changes direction as we move spatially toward roller R2. Figure 8 shows results when the roller R2 is an RPG guide roller which rotates in sinusoidal motion around a pivot point which is at a distance X_1 from R2 in the entry span; note that this also induces a roller displacement $z_L(t) = X_1\theta_L(t)$. In essence, this action mimics a combination of pure displacement and pure rotation at R2. In this case, the web slope is in the same direction as the lateral motion direction as R2 is directing motion in the entry span (note that R1 is fixed).

For the second set of numerical simulations, we consider the following scenario which often comes up in practical situations and does not have a clear answer in the literature. Does a web guide completely eliminate propagation of lateral position oscillations into downstream spans? To address this issue, we consider the setup shown in Fig. 6 with a controlled remotely pivoted guide at R2; a PI controller is often used in industry based on measurement of web lateral position on the guide roller R2. Figure 9 provides the lateral position response for different locations in the entry span. It is clear that the web guide is able to regulate the web lateral position, $y_L(t)$, to zero. This controller is able to regulate lateral position to zero at the guide roller. Further, there is no propagation of these oscillations into the exit span provided the exit span is perpendicular to the entry span, i.e., the angle of wrap on the guide roller is 90 deg. If the wrap angle is 90 deg, the rotation of the guide roller in the plane of the entry span simply twists the web in the exit span. If the wrap angle is not 90 deg, then the in-plane rotation of the guide roller is projected as an initial web slope for the exit span, resulting in twisting and bending of the web in the exit span.

Figure 10 provides the guide roller angle or control action ($\theta_L(t)$) to regulate the web lateral position at zero as shown in Fig. 9. When the wrap angle on R2 is $\beta = 89$deg, the projection of the guide roller rotation into the exit span plane is $\theta_{0R2}(t) = \theta_L(t)\cos(\beta)$ which is provided in Fig. 11; this acts as a disturbance to the exit span. Figure 12 provides the response of the lateral position and slope at different locations of the exit span due to this disturbance. Although the lateral position at the guide roller has been regulated at zero, both the web lateral position and slope at subsequent locations of the span are not zero. There is propagation of lateral oscillations into downstream spans. These typical numerical simulations illustrate the benefit of the developed spatially dependent transfer functions for understanding lateral behavior in ideal as well as nonideal situations.

6 Conclusions

In this paper, we have derived spatially dependent transfer functions for web lateral dynamics. The obvious benefits of such

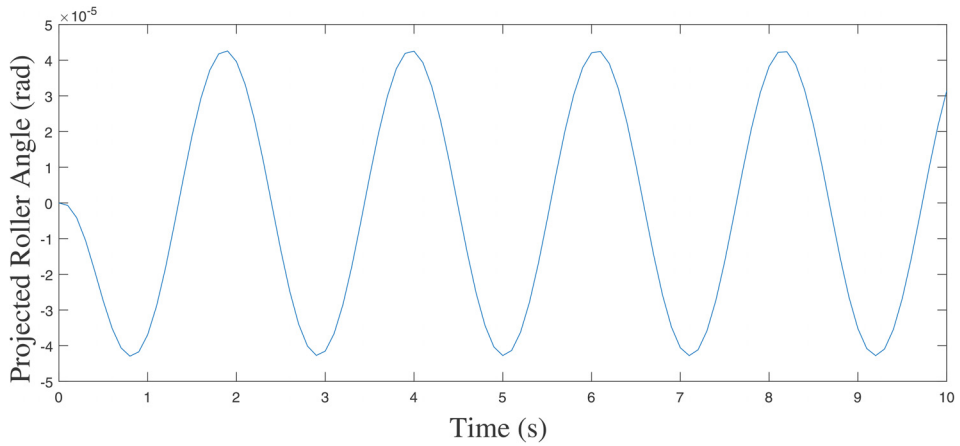

Fig. 11 Projection of the guide roller rotation into the plane of the exit span; $\theta_{0R2}(t) = (\cos\beta)\theta_L(t)$ and β is the web wrap angle on the guide roller

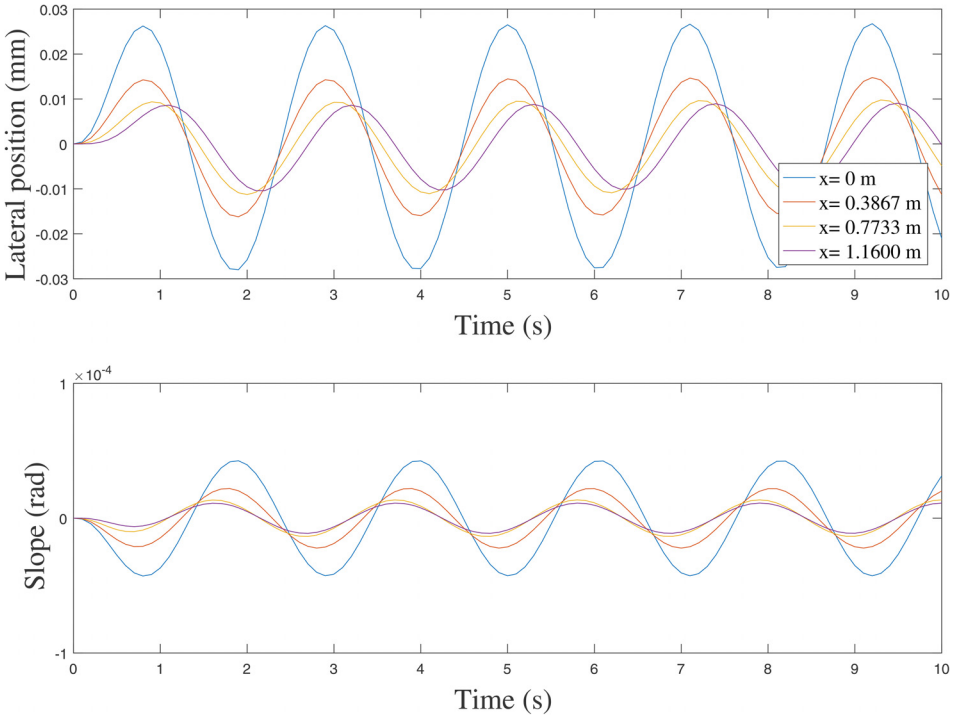

Fig. 12 Evolution of web lateral position and slope for 4 points along the exit span for 89 deg wrap angle

governing equations are that one can obtain the evolution of lateral position response at any location in the span as well as all higher-order spatial partial derivatives, such as slope, moment, shear force, etc. Further, these transfer functions may be used to control the lateral position and slope at a prescribed location in the span other than on the roller. In addition, R2R manufacturing of flexible and printed electronics requires positioning the web precisely in both lateral and longitudinal directions. Traditional printing systems have relied solely on longitudinal registration for printing presses with multiple print units. With the goal of achieving print registration accuracy within a few microns in R2R printing of electronics, this work is expected to aid in a more precise analysis of lateral behavior and facilitate the design of model-based lateral control systems for achieving tight regulation of lateral print registration. In the future, we plan to conduct experiments to validate the proposed models and design and evaluate model-based controllers.

Funding Data

- Directorate for Engineering National Science Foundation under Grant No. (1635636).

Nomenclature

A = cross-sectional area of web
E = modulus of elasticity of web material
f_k = defined functions, $k = 1, .., 3$
G = shear modulus
$g_l(x)$ = defined functions, $l = 1, 2, 3$
$g_{lx}(x)$ = first-order spatial derivatives of defined functions
$g_{lxx}(x)$ = second-order spatial derivatives of defined functions
I = web span moment area of inertia
K = constant parameter, $K^2 = T/EI$
K_e = constant parameter K with shear effect, $K_e^2 = K^2/[1 + nT/AG]$
L = web span length
m = mass per unit length
n = correction factor
N = shear force
P_m = numerator polynomial functions in transfer functions, $m = 1, .., 5$
s = Laplace variable
t = time
τ = time constant, $= L/v$
T = web tension
v = web transport velocity
v_y = web lateral velocity
x = transport direction distance
X_1 = pivoting distance from guide roller
y = web lateral displacement
z_i = roller lateral displacement
β = wrap angle
θ_i = roller angle
θ_{wi} = web angle
$\mathcal{L}\{\bullet\}$ = Laplace transform
$\tilde{\bullet}$ = shear variable that can be reduced to bending
$\hat{\bullet}(x, s)$ = transformed function

Subscripts

b = bending
i = position in the span, 0 (upstream roller) or L (downstream roller)
s = shear
t = total effect, bending, and shear

References

[1] Seshadri, A., and Pagilla, P. R., 2013, "Modeling Print Registration in Roll-to-Roll Printing Presses," ASME J. Dyn. Syst., Meas., Control, **135**(3), p. 031016.
[2] Shelton, J. J., 1968, "Lateral Dynamics of a Moving Web," Ph.D. dissertation, Oklahoma State University, Stillwater, Ok.
[3] Shelton, J. J., and Reid, K. N., 1971, "Lateral Dynamics of a Real Moving Web," ASME J. Dyn. Syst., Meas., Control, **93**(3), pp. 180–186.

[4] Shelton, J. J., and Reid, K. N., 1971, "Lateral Dynamics of an Idealized Moving Web," ASME J. Dyn. Syst., Meas., Control, **93**(3), pp. 187–192.
[5] Sievers, L., 1987, "Modeling and Control of Lateral Web Dynamics," Ph.D. dissertation, Rensselaer Polytechnic Institute, Troy, NY.
[6] Yerashunas, J. B., Abreu-Garcia, J. A. D., and Hartley, T. T., 2003, "Control of Lateral Motion in Moving Webs," IEEE Trans. Control Syst. Technol., **11**(5), pp. 684–693.
[7] Seshadri, A., and Pagilla, P. R., 2010, "Optimal Web Guiding," ASME J. Dyn. Syst., Meas., Control, **132**(1), p. 011006.
[8] Seshadri, A., and Pagilla, P. R., 2012, "Adaptive Control of Web Guides," Control Eng. Pract., **20**(12), pp. 1353–1365.
[9] Brown, J., 2005, "A New Method for Analyzing the Deformation and Lateral Translation of a Moving Web," Eighth International Conference on Web Handling, Stillwater, OK, June 5–8, pp. 39–58.
[10] Curtain, R., and Morris, K., 2009, "Transfer Functions of Distributed Parameter Systems: A Tutorial," Automatica, **45**(5), pp. 1101–1116.
[11] Benson, R. C., 2002, "Lateral Dynamics of a Moving Web With Geometrical Imperfection," ASME J. Dyn. Syst., Meas., Control, **124**(1), pp. 25–34.
[12] Brown, J., 2017, "The Effect of Mass Transfer on Multi-Span Lateral Dynamics of a Uniform Web," Fourteenth International Conference on Web Handling, Stillwater, OK, June 5–7, pp. 1–8.